Available online at www.sciencedirect.com

SCIENCE DIRECT

International Journal of Mass Spectrometry 247 (2005) 40–47

International Journal of Mass Spectrometry

www.elsevier.com/locate/ijms

Limitations of the effective potential for the evaluation of the ion energy in the RF-driven quadrupole field

V.I. Baranov*, D.R. Bandura, S.D. Tanner

MDS SCIEX, 71 Four Valley Drive, Concord, Ont., Canada L4K 4V8

Received 11 August 2005; accepted 11 August 2005
Available online 7 October 2005

Abstract

The concept of the effective potential provides inadequate estimation of the ion energy in RF-driven quadrupole fields. It is especially limited for the quantitation of additional enthalpy introduced by the RF-driven field for an ion molecule reaction. On the contrary, the effective potential is clearly successful in describing of the ion oscillation frequency, and has been surprisingly powerful considering the strict limitations of the adiabatic approximation. This work is an attempt to understand this contradiction and to consider a novel concept of the estimation of the ion energy in an RF field. This theoretical model for the averaged ion energy is useful in describing specific features of the RF field contribution to the enthalpy of ion molecule reactions. To demonstrate this effect, several ion molecule reactions are investigated experimentally including cluster formation, endothermic and exothermic oxidation reactions.

Keywords: Effective potential; RF-driven quadrupole fields; Limitations of the adiabatic approximation

1. Introduction

With the recent extensive development and acceptance of ion molecule reactors in a variety of analytical applications [1], the problem of quantitation of additional enthalpy introduced by the RF-driven field has shifted from academic dispute between ion molecule chemistry groups [2] to practical usage of commercial instrumentation. It is time to refine our concept of averaged ion energy over the full range of RF field conditions in practical use. This work is an attempt to evaluate a novel concept of the averaged ion energy in the case of the quadrupole field.

Partitioning of the ion trajectory into a smooth drift and rapidly oscillating terms, as was hypothesized in [3], has introduced the important concepts of the effective potential, safe operating conditions for RF-driven devices and stability parameterization. Such separation is equivalent to formalization of the ion movement as a superposition of two independent degrees of freedom. Although widely used, this concept is less effective in the evaluation of the ion energy in the RF-driven field under non-adiabatic conditions and corrective attempts had been made [4]. In part, this work is an attempt to understand the boundaries and accuracy of this approach. Cooling of ions by buffer gas is very complicated process, which among the other things depends on time [5]. Axial ion energy is dissipated not only by the buffer gas but also by the energy transfer into the radial component. This work describes the ion energy after ion trapped for “a long time” (as well as the effective potential approach) after complete relaxation. Therefore, only the RF field and buffer gas kinetic contributions are considered.

Direct simulation of the ion trajectory is also extensively used (for example, [6,7]) and represents a very powerful and versatile tool in the investigation of averaged characteristics of the ion flow. Despite its extensive computational requirements, it is still the most reliable modeling method for investigation of the influence of quadrupole acceptance on the ion energy. It is used here for comparative purposes and as a proxy of the experimental data, which are otherwise often difficult to acquire.

An important practical manifestation of the RF field influence on the ion energy is its quantifiable contribution to the enthalpy of an ion molecule reaction. To demonstrate the effect of the RF field on ion chemistry and verify proposed theoretical constructs, several ion molecule reactions are investigated in this work including cluster formation, endothermic and exothermic oxidation reactions.

---

* Corresponding author.
E-mail addresses: vladimir.baranov@sciex.com, vladimir.baranov@utoronto.ca (V.I. Baranov).

1387-3806/$ – see front matter © 2005 Elsevier B.V. All rights reserved.
doi:10.1016/j.ijms.2005.08.011

Table 1
Values of $\upsilon_{21}^2(a,q)$ and $\upsilon_{22}^2(a,q)$ (Eqs. (2) and (3)) for selected a and q parameters

a, q	$\upsilon_{21}^2(a,q)$	$\upsilon_{22}^2(a,q)$	$\beta(a,q)$	a, q	$\upsilon_{21}^2(a,q)$	$\upsilon_{22}^2(a,q)$	$\beta(a,q)$
0, 0.1	0.01	1.01	0.07085	0.1, 0.5	0.47	1.17	0.50930
0, 0.2	0.04	1.04	0.14255	0.1, 0.6	0.88	1.59	0.59043
0, 0.3	0.10	1.09	0.21606	0.1, 0.7	1.98	2.65	0.69518
0, 0.4	0.20	1.18	0.29257	0.1, 0.8	12.55	12.56	0.86704
0, 0.5	0.36	1.32	0.37374	−0.1, −0.5	0.53	3.71	0.15685
0, 0.6	0.63	1.57	0.46225	−0.1, −0.6	0.57	2.19	0.29708
0, 0.7	1.18	2.08	0.56307	−0.1, −0.7	0.90	2.19	0.41660
0, 0.8	2.79	3.56	0.68856	−0.1, −0.8	1.63	2.73	0.54044
0, 0.85	5.68	6.23	0.77295	0.2, 0.7	6.45	6.79	0.84549
				−0.2, −0.7	1.30	5.02	0.20474

2. Theory

It was recently suggested [8,9] that in order to evaluate the averaged ion energy in the quadrupole RF field, one can calculate two dimensionless parameters $\upsilon_{21}^2(a,q)$ and $\upsilon_{22}^2(a,q)$, which depend only on the field properties (see Table 1; some values in this Table slightly differ from [9] due to more accurate calculation of the dimensionless parameters close to the stability boundaries). Following is a short summary of results reported in [9] and definition of the symbols used.

For the two-dimensional quadrupole capacitor, the potential of the RF-driven quadrupole field can be expressed as a combination of two terms having constant (U) and periodic (V) trapping potentials:

$$\Phi = \frac{(x^2-y^2)}{2r_0^2}(U - V\cos(\omega t+\varphi)), \tag{1}$$

where $2r_0$ is the electrode separation and ω is the main trapping RF angular frequency. An ion (with mass m and charge e) having arbitrary initial conditions $\{x_i, y_i, z_i\}$, $\{\dot{x}_i, \dot{y}_i, \dot{z}_i\}$ and φ (the initial value of the phase of the main trapping frequency, which depends on the choice of the origin of time t_i) undergoes quasi-periodic motions in the quadrupole field (1). After introduction of the usual dimensionless parameters $4eU/m\omega^2r_0^2 = a$, $2eV/m\omega^2r_0^2 = q$, the equations of ion motion are significantly simplified. A comprehensive analysis of the ion motion was given in [9], where the following integrals and functions of a, q, ωt, and φ were introduced:

$$\upsilon_{21}^2(a,q,\omega t,\varphi) = \frac{(\dot{C}(a,q,(1/2)\varphi)\dot{S}(a,q,(1/2)/(\omega t+\varphi)) - \dot{C}(a,q,(1/2)(\omega t+\varphi))\dot{S}(a,q,(1/2)\varphi))^2}{(-C(a,q,0)\dot{S}(a,q,0))^2}$$
$$\upsilon_{21}^2(a,q) = \left\langle \langle \upsilon_{21}^2(a,q,\omega t,\varphi)\rangle_{\varphi} \right\rangle_{\omega t} \tag{2}$$

$$\upsilon_{22}^2(a,q,\omega t,\varphi) = \frac{(\dot{C}(a,q,(1/2)(\omega t+\varphi))S(a,q,(1/2)\varphi) - C(a,q,(1/2)\varphi)\dot{S}(a,q,(1/2)(\omega t+\varphi)))^2}{(-C(a,q,0)\dot{S}(a,q,0))^2}$$
$$\upsilon_{22}^2(a,q) = \left\langle \langle \upsilon_{22}^2(a,q,\omega t,\varphi)\rangle_{\varphi} \right\rangle_{\omega t}. \tag{3}$$

Here $C(a,q,(1/2)\,(\omega t+\varphi))$ is the even Mathieu function with real characteristic value a and parameter q and $S(a,q,(1/2)\,(\omega t+\varphi))$ is the odd Mathieu function. Their derivatives with respect to the $(1/2)\,(\omega t+\varphi)$ variable are $\dot{C}(a,q,(1/2)(\omega t+\varphi))$ and $\dot{S}(a,q,(1/2)(\omega t+\varphi))$, respectively. The parameters $\upsilon_{21}^2(a,q)$ and $\upsilon_{22}^2(a,q)$ are obtained by averaging of $\upsilon_{21}^2(a,q,\omega t,\varphi)$ and $\upsilon_{22}^2(a,q,\omega t,\varphi)$ over initial phase and time as following:

$$\text{over}\,\varphi: \quad \langle f(\varphi)\rangle_{\varphi} = \frac{1}{2\pi}\int_0^{2\pi} f(\varphi)\mathrm{d}\varphi, \tag{4}$$

$$\text{and}\,\omega t: \quad \langle f(t)\rangle_t = \lim_{T\to\infty}\frac{1}{T}\int_0^{T} f(t)\mathrm{d}t. \tag{5}$$

For the averaged ion energy in the presence of the RF field the following equations were obtained [9]:

$$\begin{aligned} E_x &= \frac{m\omega^2x_i^2}{8}\upsilon_{21}^2(a,q) + \frac{m}{4\gamma_\perp^2}\upsilon_{22}^2(a,q),\\ E_y &= \frac{m\omega^2y_i^2}{8}\upsilon_{21}^2(-a,-q) + \frac{m}{4\gamma_\perp^2}\upsilon_{22}^2(-a,-q),\\ E_r &= E_x + E_y. \end{aligned} \tag{6}$$

Terms $(m\omega^2x_i^2/8)\upsilon_{21}^2(a,q)$ and $(m/4\gamma_\perp^2)\upsilon_{22}^2(a,q)$ can be described as an averaged potential and kinetic energy, respectively. Here, the most probable ion thermal speed $1/\gamma_\perp$ is related to the initial translational kinetic temperature $T_\perp$ in the radial direction as follows:

$$\gamma_\perp^2 = \frac{m}{2k_\mathrm{B}T_\perp}. \tag{7}$$

Let us investigate the general case $\begin{cases} a \neq 0 \\ q \neq 0 \end{cases}$. In this instance the RF field contribution into the averaged ion energy is different for the x and y radial directions, because $\upsilon_{21}^2(a,q)$ and

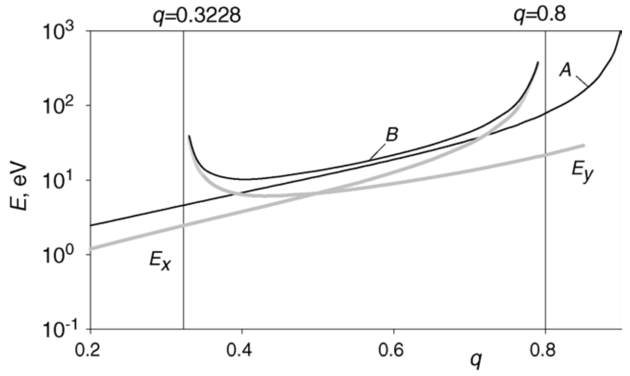

Fig. 1. Ion energy vs. the q parameter for an ion on the scan line $a = 0.1596q$. For the case considered: $\omega = 2\pi \times 10^6\,\mathrm{s}^{-1}$, $m = 250\,\mathrm{D}$, $\gamma_\perp = 10^{-3}\,\mathrm{s\,m}^{-1}$, x_i, $y_i = 0.25r_0$. E_x and E_y are the averaged ion energies for the x and y directions, respectively; (A) the radial (combination of x and y directions) ion energy for the same ion but for $a = 0$; (B) the radial ion energy between the stability boundaries corresponding to the selected scan line.

$v_{22}^2(a, q)$ are not symmetrical functions of a and q. The stability boundaries are different for the x and y directions; moreover, they belong to different values of the Mathieu characteristic exponent $\beta(a, q)$ (Eq. (15) below). On the boundary, the ion energy is very large. Let us consider the scan line $a = 0.1596q$, which intersects the stability boundary $\beta(0.12767, 0.8) = 1$ in the x direction and $\beta(-0.05151, -0.32277) = 0$ in the y direction, presented in Fig. 1. The ion energy for the radial direction (combination of both degrees of freedom) has a clear minimum that is located between the stability boundaries. In this particular case, the minimal ion energy is observed around $a = 0.064$, $q = 0.4$. Eq. (6) allows evaluation of the averaged ion energy of complex ion mixtures simultaneously present in the trap.

The overall structure of the dependence of the ion energy on the q parameter is somewhat as expected: the field contribution increases with approach to the stability boundary, where ions eventually become unstable. The instance of $q \rightarrow 0$ should be considered as a special case. Formally, this region is also close to the stability boundary. However, the RF field is negligible in comparison with the ion inertia, and instability is difficult to distinguish experimentally from severely limited acceptance (which is largely defined by geometric matching of the ion beam — quadrupole assembly pair). Also, it is apparent that for low ($q \rightarrow 0$) strength of the RF field the $v_{22}^2(a, q)$ parameter should not be less than one. In fact, this parameter should never be less than one (the radial ion motion cannot collapse completely [10]). However, for example, $v_{22}^2(0.1, 0.1) = 0.53$, which is counter-intuitive. To understand that, one should consider E_r, which is the sum of unequal contributions of both degrees of freedom. An ion trajectory is stable (the ion energy is less than infinity) when the Mathieu characteristic exponent is a real number: $\beta(0.1, 0.1) = 0.32493$, however, $\beta(-0.1, -0.1) = -0.30893i$. Therefore, this trajectory is unstable and no value for the averaged ion energy can be assigned to it. In Table 1 only instances of stable trajectories in both radial directions are considered.

To be consistent with [3,11] in estimating the energy of an ion in the quadrupole field within the first stability region, one should assume that:

$$\begin{cases} a = 0 \\ q \rightarrow 0 \\ \varphi = 0 \\ |x(t)| < r_0 \end{cases}. \tag{8}$$

The potential energy was deduced in [11] to be equal to:

$$\varepsilon_x = \frac{e^2V^2}{4m\omega^2 r_0^2}\left(\frac{x_i}{r_0}\right)^2, \tag{9}$$

per degree of freedom for the quadrupole field (assuming the definition (1) of the RF amplitude; an alternative deduction was presented in [9] and the effective potential model experimental validation in [12]). For the linear quadrupole the radial potential ion energy is given by:

$$\varepsilon_r = \frac{e^2V^2}{4m\omega^2 r_0^2}\left(\frac{r_i}{r_0}\right)^2, \tag{10}$$

where $r_i^2 = x_i^2 + y_i^2$.

On this level of approximation, it was expected that a system (an ion in effective potential field) executes small harmonic oscillations near a position of stable equilibrium with the potential energy $\varepsilon_x = (m/2)\Omega^2 x_i^2$, where Ω is the circular frequency of the oscillations. Ω is entirely determined by the properties of the system itself:

$$\Omega = \frac{eV}{\sqrt{2}m\omega r_0^2} = \frac{q\omega}{2\sqrt{2}}. \tag{11}$$

This approximation to the ion potential energy (9) and (10) is surprisingly powerful considering the strict limitations (see Eq. (8)). To demonstrate, let us evaluate the accuracy of Eq. (11) in describing the oscillation frequency. Fig. 2 represents the power spectrum of the ion trajectories in the ideal quadrupole field for $\begin{cases} a = 0 \\ q = \{0.1, 0.4, 0.7\} \end{cases}$. It is evident that for the first harmonic of the oscillation frequency, the exact (see Eq. (12) in [8]) and

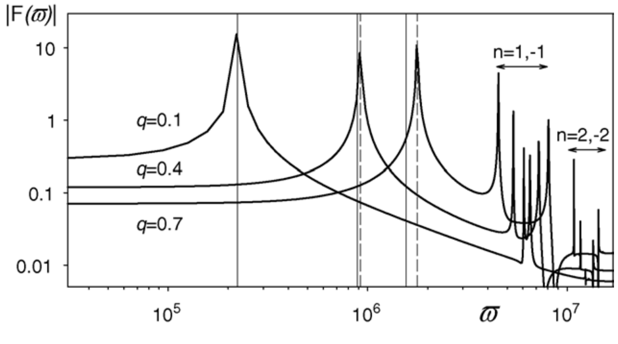

Fig. 2. Power spectrum $|F(\varpi)|$ of the ion trajectory in the ideal quadrupole field for $\omega = 2\pi \times 10^6\,\mathrm{s}^{-1}$ and $q = \{0.1, 0.4, 0.7\}$. Here ϖ is the frequency variable. The ion oscillation frequency was calculated according to Eq. (12) in [8] ($\Omega_n = \omega|n + (\beta(a, q))/2)|$, $n = 0, \pm1, \pm2, \ldots$, dashed line) and Eq. (11) (solid line). $\Omega_0 = \Omega$ is the frequency of ion secular motion. Notice that contrary to popular believe ω (the main trapping RF angular frequency) is not present in the frequency spectrum.

approximate Eq. (11) values are very close, which was also observed experimentally (see, for example, [13]). Significant deviation is observed only for $q > 0.4$. Certainly, higher order resonances ($n > 0$) cannot be described directly by Eq. (11).

Unfortunately, there is no direct way to demonstrate from first principles the separation of the ion trajectory $x(t)$ into components of a smooth drift and rapidly oscillating terms, as was hypothesized in [3]; it can only be postulated. Time averaging with Maxwell–Boltzmann (MB) ion velocity distribution function was used in [9]; both procedures discriminate against the rapidly oscillating terms. However, for the smooth drift-like oscillations the situation is different. Assuming that an ion undergoes free oscillations in the potential field (see Eq. (10)), the corresponding equation of motion has a solution that can be written as:

$$x(t) = \sqrt{x_i^2 + \frac{\dot{x}_i^2}{\Omega^2}} \cos(\Omega t + \alpha); \qquad \cos(\alpha)^{-1} = \sqrt{1 + \frac{\dot{x}_i^2}{x_i^2 \Omega^2}}. \tag{12}$$

The smooth drift term can also be presented for the case $\begin{cases} a = 0 \\ q \neq 0 \end{cases}$ as a first harmonic of the Fourier series of the ion trajectory [8,9]:

$$x(t) \sim \cos\left(\frac{\omega t}{2} \beta(0, q)\right), \tag{13}$$

and with proper choice of the origin of time, we have

$$\frac{\beta(0, q)}{2} = \frac{\Omega}{\omega}. \tag{14}$$

Here the Mathieu characteristic exponent is

$$\begin{aligned} \beta(a, q) &= \pm \frac{1}{\pi} \arccos\left(\frac{C(a, q, \pi)}{C(a, q, 0)}\right) + 2n \\ &= \pm \frac{1}{\pi} \arccos\left(\frac{\dot{S}(a, q, \pi)}{\dot{S}(a, q, 0)}\right) + 2n, n = 0, \pm 1, \pm 2, \ldots \end{aligned} \tag{15}$$

which is a rational number for a stable ion trajectory [8,9]. Isolating the case $\begin{cases} a = 0 \\ q \to 0 \end{cases}$ and in combining with Eq. (11), we have the well known approximation for the Mathieu characteristic exponent:

$$\beta(0, q) = \frac{q}{\sqrt{2}}. \tag{16}$$

Comparative graphing of the ion trajectory according to Eq. (3) in [9] (plot a) with approximations (according to Eqs. (12) and (13)) (plots c and b, respectively) is presented in Fig. 3. It is apparent that the small error in the oscillation frequency for $q = 0.4$ (panel B) diminishes with reduction of q (see panel A).

This clear success of the description of the oscillation frequency with rather simple Eqs. (11) and (12) could be explained by the fact that Ω is determined only by the system and is independent of $\{x_i, y_i, z_i\}$, $\{\dot{x}_i, \dot{y}_i, \dot{z}_i\}$ and φ. Its value is also easy to measure experimentally (see, for example, [6]). Unfortunately, this is not the case for the ion energy, which depends on the initial conditions as well as on the properties of the system itself.

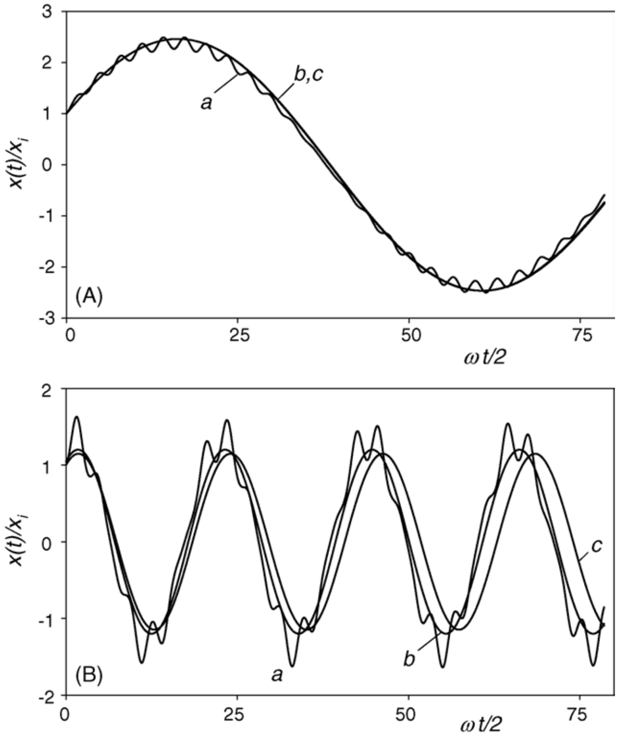

Fig. 3. The ion trajectory $x(t)/x_i$ (curve a) for $q = 0.1$ (panel A) and $q = 0.4$ (panel B) in comparison with approximation according to Eq. (13) (curve b) and Eq. (12) (curve c).

The energy of a system executing small one-dimensional oscillations is:

$$E_x = \frac{m}{2}(x_i^2 \Omega^2 + \dot{x}_i^2) \tag{17}$$

For conditions (8) employing Eq. (11) and averaging over the MB distribution analogous to Eq. (6) we have:

$$\begin{aligned} E_x &= \frac{\gamma_\perp}{\sqrt{\pi}} \int_{-\infty}^{\infty} \frac{m}{2} \left(\frac{1}{8} m\omega^2 x_i^2 q^2 + \dot{x}_i^2\right) \exp(-\gamma_\perp^2 \dot{x}_i^2) \mathrm{d}\dot{x}_i \\ &= \frac{1}{16} m\omega^2 x_i^2 q^2 + \frac{m}{4\gamma_\perp^2}, \\ E_y &= \frac{1}{16} m\omega^2 y_i^2 q^2 + \frac{m}{4\gamma_\perp^2}, \\ E_r &= \frac{1}{16} m\omega^2 r_i^2 q^2 + \frac{m}{2\gamma_\perp^2}. \end{aligned} \tag{18}$$

Direct comparison with Eq. (6) reveals that $\upsilon_{21}^2(0, q, \varphi = 0) \approx (1/2)q^2$(not averaged over φ). Different levels of $\upsilon_{21}^2(0, q, \omega t, \varphi)$ averaging were presented in [9].

Eq. (18) was developed assuming the time average values for $\varphi = 0$ only, which is not quite satisfactory. This is especially clear in the $\upsilon_{21}^2(0, q)$ dependence on the q parameter, which is much closer to $\upsilon_{21}^2(0, q) \approx q^2$ (see Table 1). Therefore, this observation implies that the definition (18) (based on the secular frequency $\Omega = \omega(\beta(0, q)/2)$ only) underestimates the potential energy of the ion oscillations by a factor of two. The rapidly oscillating part (which includes $\Omega_n = \omega|n + (\beta(a,\ q)/2)|$, $n = 0, \pm 1, \pm 2, \ldots$) of ion motion contributes equally into the potential energy at least for $q < 0.4$, which allows formal consideration of both terms as independent degrees of freedom. The situation is less clear for $q > 0.4$ where this separation cannot be justified and Eq. (6) has no equivalent. Taking the factor two into consideration, Eq. (6) is comparable to approximation (18) around $q < 0.4$, which is a well-accepted limit of the effective potential formalism.

3. Results and discussion

Direct simulation of the ion trajectories was conducted and the results are presented in Fig. 4. The procedure of the direct simulation was described in detail in [6]. Briefly, for an ion with given initial conditions, its trajectory in the ideal quadrupole field is numerically calculated according to the Mathieu equation of motion. Its energy is averaged similar to Eq. (5) for given time period (0.5 s, arbitrarily chosen). A new ion is generated with random initial conditions (including φ) within $\{0.1, 0.25, 0.5\}r_0$ annulus around the quadrupole axis. The averaged ion energy is obtained after averaging of 1000 ion trajectories. As could be seen in Fig. 4, comparing reveals no significant difference between the direct simulation and analytical result obtained via Eq. (6).

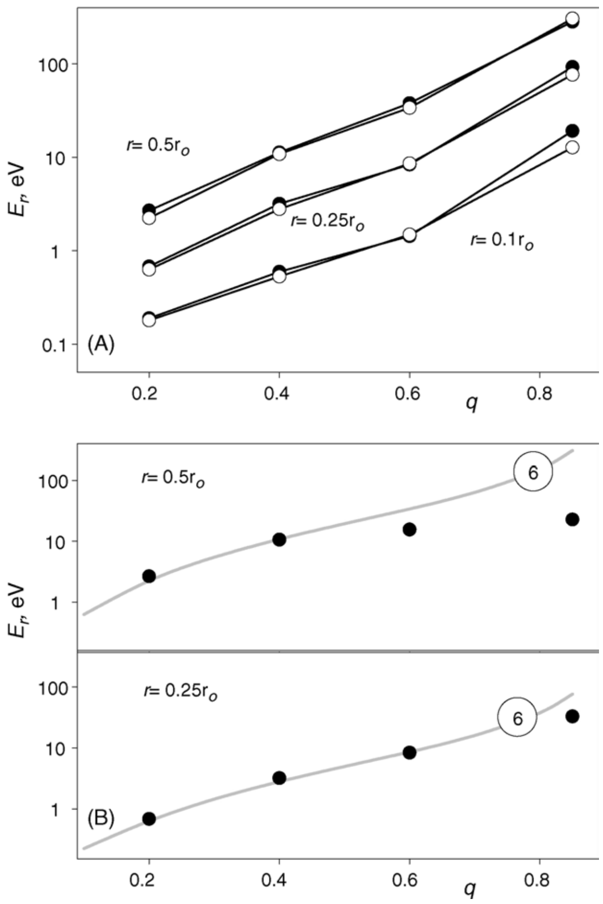

Fig. 4. Comparative plot of the averaged ion energy versus the q parameter for $\begin{cases} a = 0 \\ q \neq 0 \end{cases}$ obtained by direct simulation of the ion trajectories (closed circles) and according to Eq. (6) (open circles). For the case considered: $\omega = 2\pi \times 10^6\ \mathrm{s}^{-1}$, $m = 250\,\mathrm{D}$, $T_\perp = 1000\,\mathrm{K}$, $r = \{0.1,\ 0.25,\ 0.5\}r_o$. Panel A: all trajectories are included; panel B: only trajectories with maximum radial displacement less than r_0 are considered; (6) the averaged radial energy according to Eq. (6).

However, this is not the case if only trajectories with the maximum radial displacement of less than r_0 are taken into consideration. As can be seen in Fig. 4 panel B, the averaged ion energy for only "transmitted" or "accepted" ion trajectories is significantly different. The acceptance of the ideal quadrupole field was described systematically in detail in [8], and cannot be simplified. Comprehensive investigation of acceptance in phase space is a very challenging task. We have to limit our investigation at this point. The formalism of the effective potential does not suggest any solution for this problem either.

We speculate that in the presence of collisions, the number of transmitted trajectories is less dependent on the q parameter due to thermal relaxation of the ion beam [14] followed by radial collapse closer to the quadrupole axis (see Eq. (6), $r \to 0$). In this case the dependence of the averaged ion energy on the RF field contribution should be similar that presented in Fig. 1.

At the moment we do not have proper experimental setup to perform the state of the art quantitative measurements of the RF field energy contribution. This section should be considered as a demonstration of the most prominent features of the RF field interference with thermodynamics of ion molecule reactions, which could be observed experimentally on standard analytical equipment. We speculate that following effects should be attributed to the RF field influence and cannot be explained by formalism of the effective potential.

An increase in the contribution of the RF field to the ion energy should result in an increase in the center-of-mass energy of ion — neutral molecule collisions. Collisions do not alter the fundamental dependence (according to Eq. (6)) of ion energy on the a and q parameters since that after every collision the ion trajectory has an altered set of initial conditions. However, energy coupling between different degrees of freedom is activated by collisions.

The RF field, as an external heat source, is able to contribute enthalpy to an ion molecule reaction through frictional heating with buffer/reaction gas, suppressing some exothermic or promoting endothermic processes. It is also expected that exothermic reactions that require some additional energy to overcome an activation barrier, could be activated. For example, cluster formation occurs only on the "low energy tail" of the reactant ion energy distribution, which can be depopulated by an external heat source. On the contrary, the product of an endothermic reaction is produced from the "high energy tail" of the precursor ion energy distribution. It is feasible to distinguish between exothermic and endothermic reactions by analyzing the intensity ratio of a product ion to a reactant ion as a function of the RF field contribution. The ratio is less sensitive to variations in a reaction cell transmission. The contribution can be represented by the a and q parameters or quantified directly by E_r according to Eq. (6).

All measurements were performed with an ELAN DRC$^{\text{Plus}}$ ICP-MS instrument (Perkin-Elmer Sciex, Shelton CT) equipped with the dynamic reaction cell (DRC) — gas-filled RF-driven quadrupole operated in the first stability region. The DRC power supply provides operational control of the dc and RF trapping potentials. Carbon dioxide (Coleman Grade, 99.99%, BOC Gases) was used as a reaction gas. Operating conditions were as described elsewhere [15]. The plutonium sample was the long-lived isotope ^{242}Pu, purchased from NIST (SRM 4334G, Gaithersburg, MD), and diluted to 1 ng mL^{-1} (1 ppb) in 1% nitric acid.

The DRC is equipped with an axial or drift field, which is provided by a set of additional electrodes [16] biased to a dc potential. The axial field is not significant to provide a measurable contribution into the reaction enthalpy. On the other hand, the thermalized ion beam is expected to collapse along the quadrupole axis where the RF field contribution is not expected to be significant either (see Eq. (6)). Collisional relaxation leads to a decrease of the potential energy of ion motion (associated with $\upsilon_{12}^2(a, q)$) due to diminution of radial amplitude of the ion trajectory. The kinetic energy (associated with $\upsilon_{22}^2(a, q)$) of thermalized ions depends on the neutral gas temperature and the field and will not decrease beyond a certain limit [8,9]. However, in the presence of collisions, the coupling between axial and radial degrees of freedom leads to an increase in the amplitude of the ion trajectory, which prevents the ion beam from completely collapsing. Therefore, the axial field contributes into the enthalpy of the ion molecule reaction indirectly by increasing the RF field contribution and directly into the kinetics by a reduction of the ions' residence times inside the DRC. The result is a combined effect, which is difficult to dissect.

The DRC has a frequency scanning power supply (ω is a function of ion mass, V is constant), as opposed to the more common RF amplitude-scanning (V is a function of ion mass, ω is constant). In this case Eq. (6) (for $a = 0$) can be rewritten as:

$$\begin{aligned} E_r &= \frac{m\omega^2 r_i^2}{8}\upsilon_{21}^2(0, q) + \frac{m}{2\gamma_\perp^2}\upsilon_{22}^2(0, q) \\ &= \frac{eV}{4q}\left(\frac{r_i}{r_0}\right)^2 \upsilon_{21}^2(0, q) + k_\text{B}T_\perp \upsilon_{22}^2(0, q), \qquad (19) \end{aligned}$$

and the total ion energy, formally independent of mass, will be:

$$E = \frac{eV}{4q}\left(\frac{r_i}{r_0}\right)^2 \upsilon_{21}^2(0, q) + k_\text{B}T_\perp \upsilon_{22}^2(0, q) + \varepsilon_\text{z} + \frac{1}{2}k_\text{B}T_\text{z}, \qquad (20)$$

where ε_z and T_z are the ion beam axial energy and kinetic temperature, respectively. The direct contribution of the axial field is neglected later on. The averaged translational ion energy as a function of the q parameter calculated according to Eq. (19) is presented in Fig. 5. Note that this dependence is different from that presented in Fig. 1 due to the alternative frequency scanning mode of the DRC power supply (at $V = 200$ V). The RF field contribution increases for $q \to 0$ as a result of increasing frequency. Therefore, the DRC should have two regions of elevated averaged ion energy near the stability boundaries analogous (but not homologous!) to the amplitude-scanning mode of operation (for $a \neq 0$, see Fig. 1, curve b).

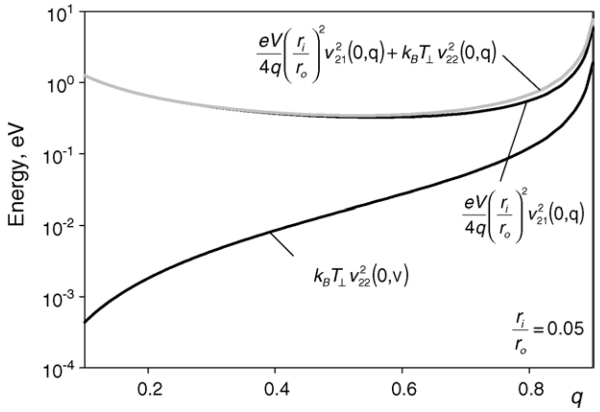

Fig. 5. The ion energy vs. q parameter according to Eq. (19) for the case of a frequency-scanned quadrupole. $r_i/r_0 = 0.05$, $V = 200$ V, $T_\perp = 500$ K.

To demonstrate the effect of the RF field on ion chemistry, several reactions were selected:

1. Formation of ammonia clusters of Zn^+ is exothermic and is electrostatic in nature. It is observed (see Fig. 6) that additional enthalpy provided by the RF field suppresses the forming of clusters close to the stability boundary of the reactant ion. Therefore, the experimental data suggests an anti-Arrhenius dependence of the rate constants for cluster formation on temperature. A decrease of ion-molecule reaction rate with increasing temperature is quite common for exothermic association reactions being a consequence of the equilibrium shift between reactant and the collision complex toward the reactant. In special cases, even entropy effects were considered to be responsible for this trend [17]. These effects allow additional suppression of cluster formation in the DRC-equipped elemental analyzer without effecting more exothermic or endothermic bimolecular ion molecule reactions.
2. Oxidation of Zn^+ by CO_2 and Co^+ by O_2 are endothermic by 4.2 and 2.3 eV, respectively. Fig. 7 demonstrates relatively low efficiency of these reactions in concordance with their

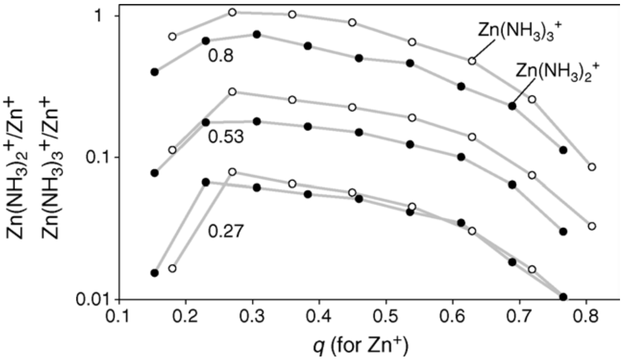

Fig. 6. Reaction of $Zn^+ + NH_3$. Ratio of ion signals of zinc–ammonia clusters to reactant Zn^+ as a function of the q parameter (for Zn^+) and ammonia flow. Three ammonia flows were used (0.27, 0.53, and 0.8 mL/min) to demonstrate extent of the ion molecule reaction. The axial field was 0.35 V/cm.

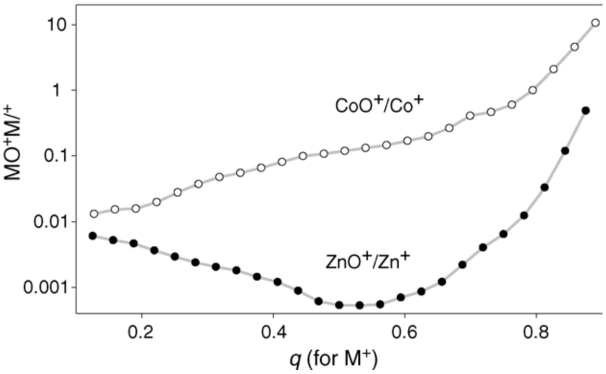

Fig. 7. Reactions of $Zn^+ + CO_2$ and $Co^+ + O_2$. Ratio of ion signals of metal oxides (MO^+) to reactant ion M^+ as a function of the *q* parameter (for M^+). Here M = Zn and Co. The axial field was 0.35 V/cm and reactant gas flows were 0.5 mL/min CO_2 and 0.57 mL/min O_2.

endothermicity. Moreover, the dependence of ZnO^+/Zn^+ as a function of the q parameter mimics the RF field contribution trend rather successfully. Reaction between Co^+ and oxygen requires less energy for promotion and one can observe that some other processes could contribute to the efficiency of this ion molecule reaction. We speculate that this trend is due to the contribution of the collision energy prior to ion thermalization in the reaction cell. This contribution to the overall enthalpy is relatively higher (compared to the RF contribution at low *q*) for reaction of Co^+ with oxygen. Despite that, Fig. 7 strongly suggests an Arrhenius dependence of the rate constants for oxide formation, with clear acceleration close to the $q \to 0.9$ stability boundary.

3. Oxidation of Pu^+ by CO_2 is exothermic by 20 or 36 kcal/mole depending on the bond dissociation energy assumed for PuO^+ [18]. It was observed [18] that the efficiency of the reaction under thermal conditions is low. This has been explained in part to the activation energy required to promote a 5f electron to 6d (1.087 eV) and in part to the significant rearrangement required for the reaction to proceed. Oxidation of U^+ by CO_2 is exothermic, requires only 0.04 eV to promote a 7s electron to 6d, and is observed [18] to proceed with higher efficiency.

Fig. 8 provides the ratio of PuO^+/Pu^+ as a function of the *q* parameter at three different flows (0.25, 0.5 or 0.85 sccm) of CO_2 and an axial field of 0.35Volts/cm. Without reaction gas, the PuO^+ signal is about 1% of the Pu^+, apparently the extent of oxide formation in the ICP source. However, when CO_2 is used as a reaction gas, the minimum PuO^+ signal observed is approximately the same as the Pu^+ signal; as in the case of Co^+ reaction with oxygen, this can been explained by the contribution of the collision energy prior to ion thermalization in the reaction cell [15]. As the value of *q* is increased, the ratio PuO^+/Pu^+ increases. With 0.25 sccm CO_2 flow, this increase in ratio continues until the signals are lost at $q \to 0.9$. For CO_2 flow >0.25 sccm, the ratio increases rapidly in the $q > 0.8$ region, and more rapidly for higher CO_2 density in the cell. Notably, this increase at $q > 0.8$ is less pronounced when the applied axial field is low, which also leads to low RF field contribution. On the contrary, U^+ reacts with CO_2 as a typical exothermic ion molecule reaction with weak dependence on the external enthalpy source. The UO^+/U^+ ratio is almost three orders of magnitude larger than the PuO^+/Pu^+ for all *q* values indicating a very efficient reaction.

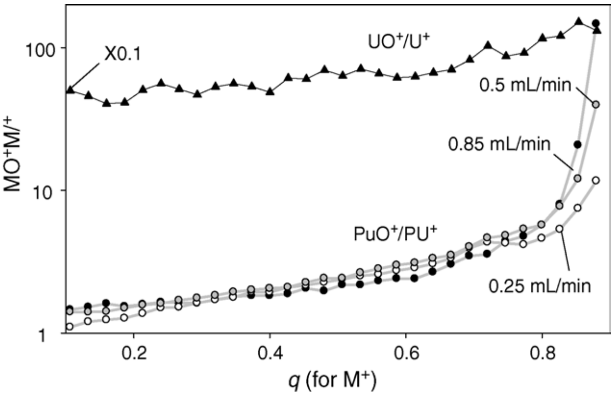

Fig. 8. Reactions of $Pu^+ + CO_2$ and $U^+ + CO_2$. Ratio of ion signals of metal oxides (MO^+) to reactant ion M^+ as a function of the *q* parameter (for M^+). Here M = Pu and U. Three CO_2 flows were used (0.25, 0.5, and 0.85 mL/min) for reaction with Pu^+. The axial field was 0.35 V/cm for data represented by circles. Closed triangles represent U^+ reaction with CO_2 (0.25 mL/min) with axial field 0.35 V/cm.

4. Conclusions

Careful theoretical, numerical modeling and simple experimental considerations confirmed that the effective potential is inadequate in description of the RF field effects on the ion molecule reactions. A novel theoretical model for the averaged ion energy, albeit more complicated in practical handling, has been proposed and confirmed qualitatively to be useful in describing specific features of the RF field contribution to the enthalpy of ion molecule reactions. Quantative verification of the model will be reported in future publications.

Acknowledgements

The Author would like to thank Frank Londry for helpful discussions, suggestions and support, Yoko Kishi for the experimental data on Zn^+ cluster formation with ammonia and Chunsheng Li and Vladimir Vais of Health Canada, Radiation Protection Bureau, for donation of the plutonium sample.

References

[1] S.D. Tanner, V.I. Baranov, D.R. Bandura, Spectrochim. Acta Part B-Atom. Spectrosc. 57 (2002) 1361.

[2] D. Schroder, H. Schwarz, D.E. Clemmer, Y.M. Chen, P.B. Armentrout, V.I. Baranov, D.K. Bohme, Int. J. Mass Spectrom. Ion Process. 161 (1997) 175.

[3] D. Gerlich, Inhomogeneous RF fields: a versatile tool for the study of processes with slow ions, in: Ng, C.-Y., Baer, M. (Eds.), State-Selected and State-to-State Ion-Molecule Reaction Dynamics. Part l. Experiment, Adv. Chem. Phys. Ser., vol. LXXXII, John Wiley & Sons, 1992, pp. 1–176.

[4] M. Schubert, I. Siemers, R. Blatt, Appl. Phys. B-Photophys. Laser Chem. 51 (1990) 414.

[5] Y. Moriwaki, M. Tachikawa, Y. Maeno, T. Shimizu, Jpn. J. Appl. Phys. Part 2-Lett. 31 (1992) L1640.
[6] F.A. Londry, J.W. Hager, J. Am. Soc. Mass Spectrom. 14 (2003) 1130.
[7] B.A. Collings, W.R. Stott, F.A. Londry, J. Am. Soc. Mass Spectrom. 14 (2003) 622.
[8] V.I. Baranov, J. Am. Soc. Mass Spectrom. 14 (2003) 818.
[9] V.I. Baranov, J. Am. Soc. Mass Spectrom. 15 (2004) 48.
[10] F.G. Major, H.G. Dehmelt, Phys. Rev. 170 (1968) 91.
[11] H.G. Dehmelt, Adv. Atom. Mol. Phys. 3 (1967) 53.
[12] R.F. Wuerker, H. Shelton, R.V. Langmuir, J. Appl. Phys. 30 (1959) 342.
[13] N.V. Konenkov, L.M. Cousins, V.I. Baranov, M.Y. Sudakov, Int. J. Mass Spectrom. 208 (2001) 17.
[14] D.J. Douglas, J.B. French, J. Am. Soc. Mass Spectrom. 3 (1992) 398.
[15] S.D. Tanner, C. Li, V. Vais, V.I. Baranov, D.R. Bandura, Anal. Chem. 76 (2004) 3042.
[16] D.R. Bandura, V.I. Baranov, S.D. Tanner, J. Am. Soc. Mass Spectrom. 13 (2002) 1176.
[17] G. Innorta, S. Torroni, A. Maranzana, G. Tonachini, J. Organomet. Chem. 626 (2001) 24.
[18] P. Santos, J. Marcalo, A.P. deMatos, J.K. Gibson, R.G. Haire, J. Phys. Chem. A 106 (2002) 7190.